



OPEN Sustained release and efficacy of Kn2-7-loaded chitosan nanoparticles under low pH conditions

Bonke Phathekile^{1,2}, Nicole Remaliah Samantha Sibuyi^{2,3},
Samantha Meyer^{2,4}, Abram Madimabe Madiehe^{2,5}, Grace Emily Okuthe⁶,
Martin Opiyo Onani¹ & Mervin Meyer²

Delivery of antimicrobial peptides to low-pH sites is a significant challenge, and results in reduced treatment efficacy for vaginal infections. Chitosan nanoparticles (CNPs) could be ideal vehicles for drugs to acidic pH environments and sustain their therapeutic effects. CNPs were synthesized using the ionic gelation technique and loaded with Kn2-7 peptide. The CNPs were characterized by dynamic light scattering, Fourier transform infrared spectroscopy, high-resolution transmission and scanning electron microscopes. The stability and antibacterial effects of Kn2-7-loaded CNPs were evaluated at low and normal pH levels. The CNPs had a size distribution of 327–416 nm and a zeta potential of 9.61–23.9 mV. The size distribution (340.2–753.7 nm) and Zeta potential (15.9–67.7 mV) of CNPs changed after loading Kn2-7. The CNPs loading capacity and Kn2-7 entrapment efficiency were 35.6% and 78.3%, respectively. The Kn2-7-CNPs were not stable at low-pH and released Kn2-7 instantly; however, stabilization of Kn2-7-CNPs with poly (acrylic acid) (PAA) and tripolyphosphate (TPP) increased their stability and sustained Kn2-7 release at acidic pH. The Kn2-7-CNPs_1 mg/mL TPP-PAA inhibited the growth of *Staphylococcus aureus* at pH 3.8 better than the Kn2-7 alone. Therefore, the Kn2-7-CNPs_1mg/mL TPP-PAA could serve as a promising candidate for protecting and delivering drugs in low-pH environments.

Keywords Antimicrobial peptides, Chitosan nanoparticles, Kn2-7 peptide, Microbicides, Sexually transmitted infections

Many viruses can be transmitted from one person to the next during sexual contact or intercourse, examples include human immunodeficiency virus (HIV), human papillomavirus, hepatitis B, herpes, syphilis, chlamydia, and gonorrhoea. Sexually transmitted infections (STIs) can cause long-term health problems, particularly in women and infants. The transmission of STIs can be prevented by the topical application of microbicides in the vagina or rectum before sexual intercourse¹. Microbicides are promising tools for the prevention of STIs transmission², and could mitigate the spread of infections by eliminating these pathogens upon contact¹. However, the acidic environment of the upper vagina, presents a challenge for many microbicidal agents³, many of which are denatured at pH below 5 and neutralizing their antimicrobial activity⁴. Furthermore, cervical mucus acts as a barrier to the cervix, potentially impacting the distribution and effectiveness of microbicidal agents within the vagina and cervix⁵, this renders the microbicides inefficient in the management and treatment of infectious organisms. There are various formulations of vaginal microbicides, including tablets, surfactants, films, gels, and ring microbicides. All of these formulations have failed in clinical trials due reduced bioavailability and stability, therefore high dosages will be required, which might induce adverse effects⁶. Therefore, it is postulated

¹Organometallics and Nanomaterials, Department of Chemical Sciences, University of the Western Cape, Bellville, South Africa. ²DSTI/TIA Nanotechnology Platform, Department of Biotechnology, University of the Western Cape, Bellville, South Africa. ³Health Platform, Advanced Materials Division, Mintek, Randburg, Gauteng, South Africa. ⁴Phytotherapy Research Group, Department of Biomedical Sciences, Faculty of Health and Wellness Sciences, Cape Peninsula University of Technology, Cape Town, South Africa. ⁵Nanobiotechnology Research Group, Department of Biotechnology, University of the Western Cape, Bellville, South Africa. ⁶Department of Biological and Environmental Sciences, Walter Sisulu University, Mthatha, South Africa. ✉email: nsibuyi@uwc.ac.za; monani@uwc.ac.za; memeyer@uwc.ac.za

that nanomaterial-based delivery systems can help sustain the stability of these microbicides when used under low acidity and high mucus content environments; to enhance their bioavailability and biodistribution in these hard-to-reach environments⁷. Nanomaterials with diameters of 1–1000 nm can effectively traverse mucus membranes, remain stable and accumulate in acidic environments, and allow for the controlled release of microbicidal agents. CNPs are among the organic nanomaterials that have been previously demonstrated to have mucus-penetrating properties⁸, to be able to withstand acidic environments and degrade at a slower pace, thereby allowing slow release of their cargoes. This is a desirable attribute for drug delivery systems for application in harsh environments, to retain or enhance the activity of anti-STI agents.

Antimicrobial peptides (AMPs), whether synthetic or naturally derived, exhibit a wide range of activity against bacteria, fungi, and viruses. These naturally occurring host-defense peptides, produced by various organisms including bacteria, fungi, and plants, have garnered significant interest due to their antimicrobial properties and potential to combat drug-resistant microbes^{9,10}. Kn2-7¹¹ and human β -defensin3 (H β d-3)¹² are examples of AMPs that have been shown to inhibit the growth of STIs, suggesting their potential use as microbicides. However, their susceptibility to degradation in acidic pH environments limit their application as microbicidal agents. CNPs emerge as nanocarriers of choice for delivery of AMPs in intravaginal sites and offer potential to develop more effective microbicides that are resistant to inactivation by low pH, can efficiently penetrate the mucus-rich vaginal environment and control release of the antimicrobial agents. The CNPs loaded with these peptides could, for example, be incorporated into a vaginal formulations and used as vaginal microbicides that can be topically applied within the vagina to prevent or treat microbial infections¹³. Therefore, the current research aimed to synthesize CNPs loaded with Kn2-7 (Kn2-7-CNPs) that are functional at low pH environments that simulate the vaginal environment. The stability and the prolonged release of Kn2-7 peptide were examined at acidic and basic pH. Additionally, the antibacterial effect of Kn2-7-CNPs against *S. aureus* at low and high pH levels were evaluated to determine their potential as a delivery system for antimicrobial agents for the prevention and treatment of vaginal infections.

Results and discussion

STIs have existed as long as humankind, and their treatment involves the use of microbicidal agents. Of the treatments involving the vaginal route, the major challenge arises from the vaginal environment, which is highly barricaded by the mucosal immune system. Delivery of microbicides in this environment poses a significant challenge due to biodegradation and an insufficient amount of drugs that reaches the organisms to kill the microbes. To achieve an adequate response, higher doses that are detrimental to the resident and surrounding cells may need to be used. NPs have demonstrated a massive role in transporting any type of drug to the target cells with reduced bystander effects¹⁴, and have been explored as delivery vehicles for AMPs¹⁰. Among the organic nanomaterials, CNPs produced from a natural polysaccharides¹⁵ has drawn medical attention as a drug delivery agent to cells that are part of mucosal membranes because of chitosan's water solubility, muco- and bio-adhesive properties¹⁶. Chitosan and chitosan-based NPs could be ideal delivery agents for therapeutic agents in low pH environments, where they can be degraded slowly to release the drugs at the desired site and rate. The main advantage of chitosan over other equivalent drug delivery excipients is its favorable toxicological profile. Chitosan is commonly regarded as a non-toxic, non-irritant material and has been approved for use in cosmetics and as a food supplement in several countries¹⁷. This polymer is biocompatible and biodegradable and is widely used as a pharmaceutical excipient in a range of formulations such as powders, tablets, emulsions, and gels¹⁸.

Synthesis and characterization of Kn2-7-CNPs

The KN2-7-CNPs were synthesized by cross-linking chitosan with TPP, and both the unloaded and AMP-loaded CNPs were stabilized with PAA as highlighted in Fig. 1. The formation of the unloaded (CNPs) and Kn2-7-loaded CNPs (Kn2-7-CNPs) was also confirmed by SEM, and FTIR. Characterization of NP size and morphology is crucial for understanding their behavior and performance. Dynamic light scattering (DLS) and

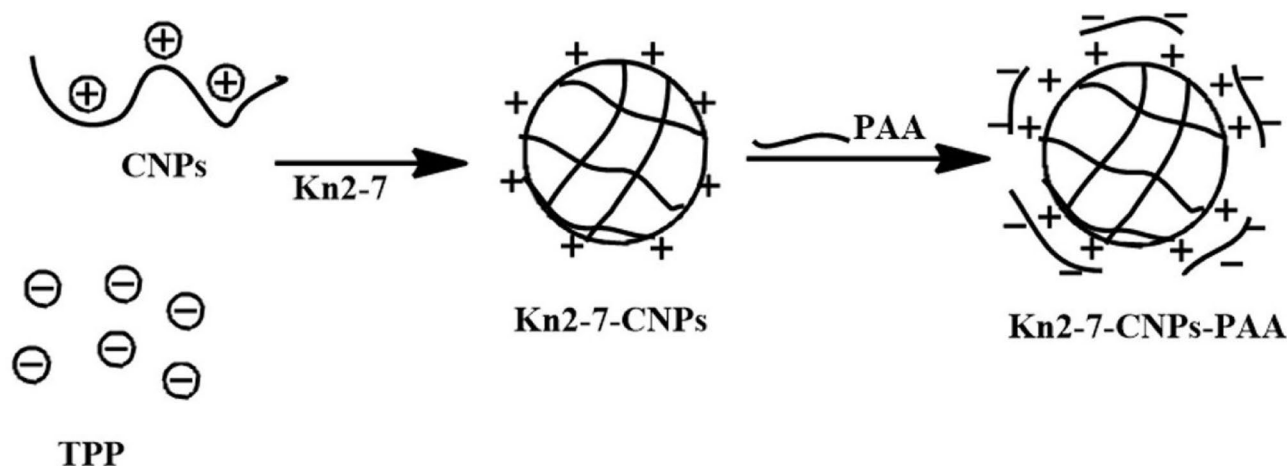


Fig. 1. Synthesis of PAA-stabilized Kn2-7-CNPs by the layer-by-layer technique²³.

[TPP] (mg/mL)	% Chitosan		Particle size (nm)		PDI		Zeta potential	
	CNPs	Kn2-7-CNPs	CNPs	Kn2-7-CNPs	CNPs	Kn2-7-CNPs	CNPs	Kn2-7-CNPs
0.3	2	0.5	327.9 ± 170.0	495.0 ± 282.3	0.592 ± 0.104	0.501 ± 0.001	9.61 ± 7.18	15.9 ± 7.50
1	2	0.5	416.7 ± 96.34	289.0 ± 152.7	0.540 ± 0.116	0.341 ± 0.045	24.9 ± 2.69	54.3 ± 6.59
2	2	0.5	382.0 ± 118.4	340.2 ± 263.4	0.293 ± 0.009	0.365 ± 0.019	21.3 ± 2.91	46.6 ± 7.79

Table 1. Particle size, PDI and zeta potential of CNPs and Kn2-7-CNPs without PAA.

CNPs	Size (nm)	PDI	Zeta Potential (mV)
Kn2-7- CNPs_1mg/mLTPP-PAA	997 ± 62.21	0.840 ± 0.043	+ 37.2 ± 5.24

Table 2. Physico-chemical properties of Kn2-7-CNPs_1mg/mLTPP-PAA.

High-Resolution Transmission Electron Microscope (HRTEM) assess the physicochemical properties of NPs that provide complementary but distinct information: DLS measures the hydrodynamic diameter of particles in their solvated state, encompassing the core, any surface coatings, and the surrounding hydration layer. In contrast, HRTEM displays the core size and morphology of individual NPs, typically revealing the electron-dense material. DLS is also highly sensitive to the presence of aggregates, as these larger structures scatter light disproportionately, often leading to significantly larger diameters even if the primary particles core sizes are small¹⁹.

DLS analysis

The light scattering effects and ζ -potential of free CNPs and Kn2-7-CNPs prepared using increasing concentrations of TPP are summarized in Table 1. The hydrodynamic diameters of the CNPs at 0.3 mg/mL, 1 mg/mL, and 2 mg/mL of TPP were 327 nm, 416 nm, and 382 nm, respectively. This is consistent with findings by previous studies which demonstrated that the physical properties of CNPs were determined by the ratio of chitosan to TPP. These sizes were similar to the sizes of CNPs produced by crosslinking of chitosan with various di- and tricarboxylic acids (succinic acid, malic acid, tartaric acid, and citric acid) in a condensation reaction with 1-[3-(dimethylamino)propyl]-3-ethyl carbodiimide methiodide²⁰.

The PDI values of unloaded CNPs were between 0.293 and 0.592; while unloaded CNPs cross-linked with 2 mg/mL of TPP and Kn2-7-CNPs crosslinked with 1 and 2 mg/mL TPP had PDI values of 0.341 and 0.365 and within ranges often associated with moderate colloidal stability (≤ 0.5). Stability can be challenged by environmental factors and subsequent coating processes^{21–23}. The high Zeta potential values of the Kn2-7-CNPs indicated that they were least stable compared to unloaded CNPs. From the literature, only NPs with Zeta potentials within the + 30 to –30 mV range are considered stable, this will help achieve AMP sustained release and prolonged residence time of the CNPs in acidic pH environments and mucosal sites. The DLS suggested that the CNPs were polydispersed, which is based on the PDI values²⁴. This observation could be attributed to the presence of two high-molecular-weight polymers (chitosan and TPP), as well as the effect of the freeze-drying process. It should also be noted that the Zeta potential for Kn2-7-CNPs-1 mg/mLTPP was 54.3 mV, and it decreased to 37.2 mV after the CNPs were coated with PAA (Table 1). The PDI also increased from 0.341 to 0.840, which may be attributed to the presence of PAA, indicating significant polydispersity and increased aggregation, thereby reflecting less colloidal uniformity for the coated NPs (Table 2).

HRTEM analysis

HRTEM analysis was used to examine the shape and core size distribution of CNPs. Figure 2 shows the varying sizes of CNPs and Kn2-7-CNPs at 1 mg/mL TPP. The HRTEM micrograph for unloaded CNPs (Fig. 2a) showed mono-dispersed spherical NPs with a size range of 2–8 nm, while the Kn2-7-CNPs-1 mg/mLTPP were polydispersed with various CNP shapes (Fig. 2b). This suggested that both peptide loading and subsequent PAA coating contributed to morphological and size heterogeneity. The core size was significantly smaller than the hydrodynamic size measured by DLS, a disparity primarily explained by the fact that DLS measures solvated particles and their aggregates, while HRTEM only focus on the core¹⁹. The size difference strongly suggested the presence of NP aggregation in solution, including for the uncoated CNPs. Banerjee et al.²², obtained spherical CNPs with a size or diameter range of 75 nm, 110 nm, and 50–600 nm using the ionic gelation method. The size differences depended on the amount of the crosslinker (glutaraldehyde) used, at 10%, 30%, and 100%, which clearly confirmed that the amount of the crosslinker influences the size of the CNPs. The shapes and sizes of CNPs can also be affected by their cargoes; the size usually increases after drug-loading. Dounighi et al. obtained spherical homogenous morphology of about 150 nm, the size increased to approximately 350 nm after loading scorpion venom into CNPs²³. Past studies confirmed that the observed hydrodynamic sizes at 300–700 nm range are indicative of the particles' behavior in solution, and suitable for biological applications, dictating their interactions within the aqueous biological environment^{25,26}.

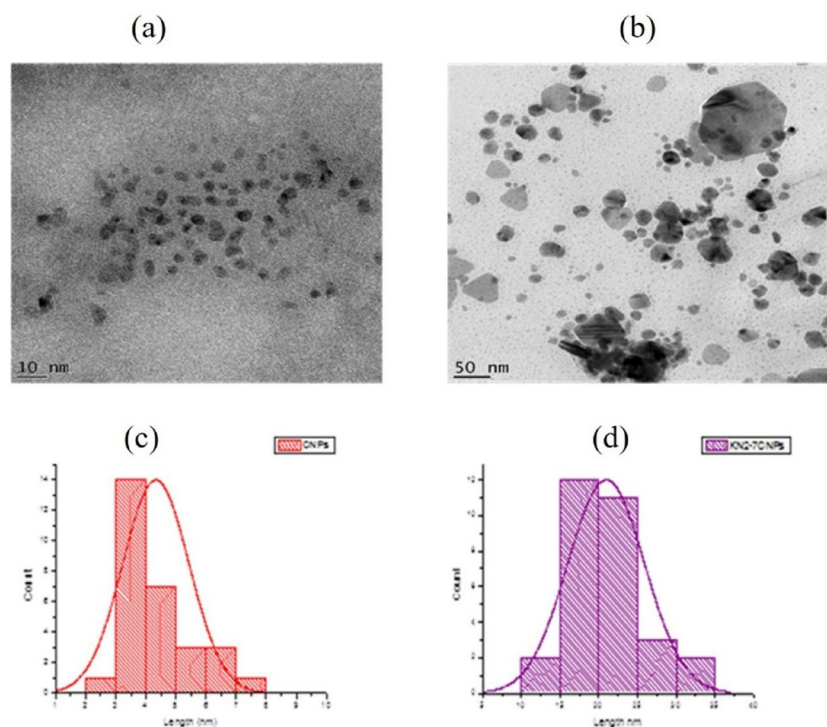


Fig. 2. HRTEM micrographs and size distribution of CNPs_1mg/mLTPP (a, c) and Kn2-7-CNPs_1mg/mLTPP (b, d), respectively.

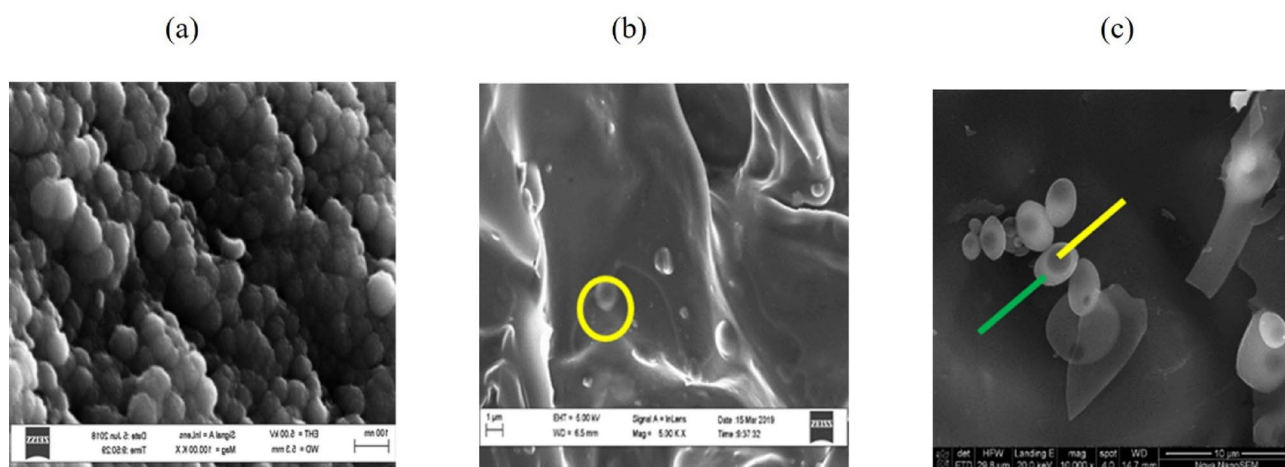


Fig. 3. SEM images for (a) CNPs_1mg/mLTPP, (b) Kn2-7-CNPs and (c) Kn2-7-CNPs_1mg/mLTPP-PAA. PAA served as a coating agent represented by a green line, while Kn2-7-CNPs was encapsulated inside the CNPs (yellow).

SEM analysis

SEM provides information about the surface, size, and the morphology of the test samples²⁷. The SEM images for unloaded CNPs or CNPs_1mg/mLTPP (Fig. 3a) showed spheroidal-shaped CNPs with smooth surfaces. The CNPs_1mg/mLTPP had a smaller size than the Kn2-7-CNPs (Fig. 3b) and Kn2-7-CNPs_1mg/mLTPP (Fig. 3c), possibly due to the loading of the peptide. Kiill et al. reported on the CNPs crosslinked with TPP that had a spherical shape, smooth surfaces, and also a homogeneous particle size distribution in the range of 70–100 nm²⁸. Hasheminejad and co-workers also reported on the spherical CNPs with sizes ranging between 129 and 148 nm, characterized by Field Emission SEM²⁹. On the contrary, Amidi and co-workers reported that the loading of protein did not affect the size and morphology of the CNPs³⁰. The current study clearly demonstrated that loading the Kn2-7 peptide altered the properties of the CNPs and their morphology. The CNPs were successfully coated with PAA (Fig. 3c) in the oval-shaped Kn2-7-CNPs with different layers shown by colored lines.

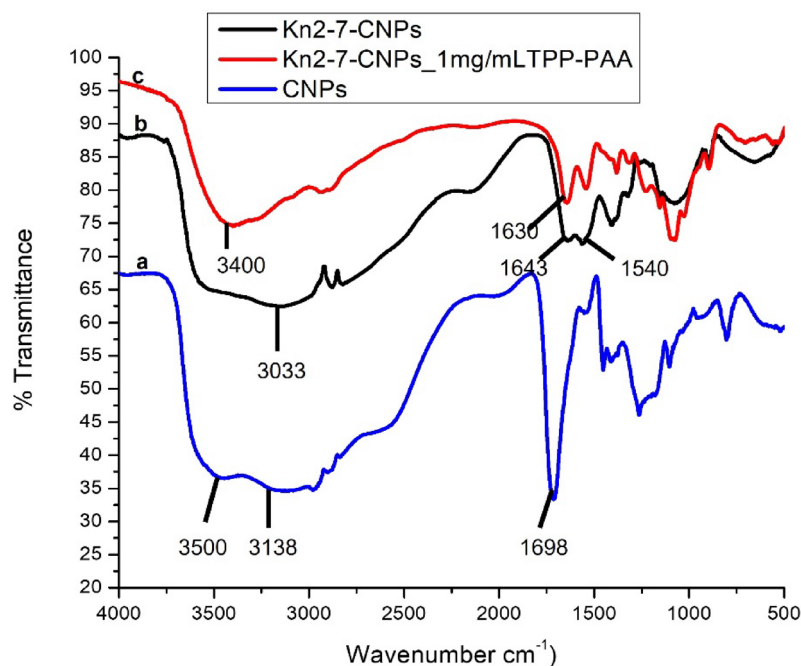


Fig. 4. FTIR spectra of (a) CNPs_1mg/mLTPP-PAA (b) Kn2-7-CNPs_1mg/mLTPP and (c) Kn2-7-CNPs_1mg/mLTPP-PAA.

Wavenumber		Vibration	Functional groups		Shift
Kn2-7-CNPs	Kn2-7-CNPs-PAA		Kn2-7-CNPs	Kn2-7-CNPs-PAA	
3400	3033	Stretching vibration	O-H, N-H	O-H, N-H	Yes
2929	2980	Asymmetric stretch	C-H	C-H	Yes
1643	1713	Bending vibration	COO ⁻	COO ⁻	New peak
1540	1453	Carbonyl stretch	CN	CN	Yes
1381	1376	Stretching	C-H (CH ₂), OH	C-H (CH ₂), OH	New peak
1226	1265	Stretching vibrations	P=O	P=O	Yes

Table 3. FTIR results for CNPs, Kn2-7 CNPs.

FTIR analysis

Figure 4; Table 3 illustrate shifts and new peaks in the FTIR spectra of Kn2-7-CNPs_1mg/mLTPP-PAA compared to CNPs_1mg/mLTPP-PAA, indicating the presence of Kn2-7 and PAA. The absorption peak at 3033 cm⁻¹ in the Kn2-7-CNPs_1mg/mLTPP-PAA spectrum corresponds to the O-H stretch from the carboxyl groups of PAA. The C-H stretching of the methyl group was observed at 2984 cm⁻¹. The decrease in the characteristic C = S peaks at 1645 and 1553 cm⁻¹ coupled with the emergence of a new band at 1713 cm⁻¹ suggests the presence of carboxyl groups from PAA. Furthermore, the broad peak at 2669 cm⁻¹ confirms the presence of NH₃⁺ in the Kn2-7-CNPs_1mg/mLTPP-PAA. The absorption peaks at 1453 and 1416 cm⁻¹ are attributed to the asymmetric and symmetric stretching vibrations of the carboxylate anion (COO⁻) groups, respectively. The peak at 1397 cm⁻¹ corresponds to CH₂ groups, consistent with findings reported by Khan et al. in their research on PAA-chitosan hydrogels for targeted colon delivery³¹. The shift of P = O peaks to 1260 and 1265 cm⁻¹ was observed in both spectra, which confirmed that this coating did not affect the crosslinking. These results suggest that the carboxyl groups of PAA dissociated into carboxylate ions (COO⁻), which then interacted electrostatically with the protonated amino groups of chitosan, forming a polyelectrolyte complex during the mixing process. The observed differences in exothermic peaks between the physical mixture and CNPs_1mg/mLTPP-PAA further support the formation of new chemical bonds upon coating Kn2-7-CNPs with PAA. These results suggested that the carboxyl groups of PAA dissociated into carboxylate ions (COO⁻), which then interacted electrostatically with the protonated amino groups of chitosan, forming a polyelectrolyte complex during the mixing process. This interaction is key to PAA's role in stabilizing the NPs and mediating their pH-responsive and mucoadhesive properties relevant for vaginal delivery.

[TPP] mg/mL	%EE	%LC
	Kn2-7-CNPs_1mg/mLTPP-PAA	Kn2-7-CNPs_1mg/mLTPP-PAA
0.3	50.7 ± 0.819	38.3 ± 0.603
1	78.3 ± 0.603	35.6 ± 0.361
3	55.6 ± 0.850	46.9 ± 1.601

Table 4. %EE and %LC values of Kn2-7 peptide in the CNPs.

pH	Time (hrs)	Temperature	[Kn2-7] µg/mL
3.8	0	Room temperature	0
3.8	24	37 °C	48
4.2	0	Room temperature	0
4.2	24	37 °C	53.2

Table 5. Stability of Kn2-7-CNPs_1mg/mLTPP-PAA in low pH conditions.

Rationale for PAA selection and future considerations

While PAA's advantages for controlled release and mucoadhesion in the vaginal environment are compelling, we acknowledge that the specific molecular weight of PAA used in this study (10000 Daltons) and the resulting coating thickness were not explicitly detailed or systematically optimized. These parameters significantly influence the steric stabilization, surface charge density, interaction with biological molecules, and subsequent behavior within mucosal barriers²⁶. Although the large hydrodynamic diameters measured by DLS indirectly suggest a substantially hydrated polymer layer, direct quantitative measurements of coating thickness (via cryo-TEM or small-angle X-ray scattering) needs to be investigated for confirmation. The impact of the PAA coating on NP–mucus and NP–cell interactions is also required. PAA's mucoadhesive nature is beneficial for drug retention, but its interaction with cellular surfaces (mediated by the altered zeta potential) needs further investigation to understand uptake mechanisms and potential cytotoxicity^{32,33}. We recognize that a comprehensive understanding requires a systematic evaluation of these interactions. Future work will systematically investigate the influence of PAA molecular weight and coating density on the physicochemical properties, stability profile across varying pH conditions, and *in vitro* and *in vivo* biological performance of the Kn2-7-CNPs-PAA. Furthermore, comparative studies utilizing alternative biocompatible polymeric stabilizers like polyethylene glycol for “stealth” properties, or other mucoadhesive polymers would provide valuable insights into optimizing the formulation for enhanced antimicrobial efficacy and reduced side effects. This will allow for a more robust justification and selection of the optimal polymer for our delivery system.

Loading capacity (%LC) and encapsulation efficiency (%EE) of Kn2-7 in CNPs

The Kn2-7 peptide was successfully incorporated into the CNPs, as shown by differences in the physicochemical properties of Kn2-7-loaded CNPs compared to those of free CNPs. The %EE and %LC values of Kn2-7-CNPs were 78.3% and 35.6%, respectively (Table 4). The %LC and %EE of Kn2-7 in the CNPs-TPP were more successful at 1 mg/mL of TPP, while 0.5 and 3 mg/mL TPP showed poor loading and encapsulation efficiency of Kn2-7 peptide due to the competition between TPP and AMPs for the same positively charged sites on the chitosan³⁴.

Release of Kn2-7 peptide from Kn2-7-CNPs in low pH conditions

The stability of the Kn2-7-CNPs_1mg/mLTPP-PAA was evaluated to demonstrate how they will behave in different pH environments, particularly at low pH levels that simulate vaginal conditions. This test was done to determine how long the peptide will be retained inside the Kn2-7-CNPs_1mg/mLTPP-PAA before their release. This study will give an estimation of the residence time of the Kn2-7 peptide inside the CNPs at low pH, and the amount of the peptide that will be released over 24 h. In the current study, Kn2-7-CNPs_1mg/mLTPP-PAA was subjected to a pH of 3.8 and 4.2 for 24 h, and the Kn2-7 release profile was evaluated by quantifying its concentration using the Qubit protein assay kit. The CNPs were sonicated with no observation of any disintegration at the tested pH at baseline (0 h) (Table 5). This indicated that Kn2-7-loaded CNPs were stable in weak acids and basic environments. However, the Kn2-7 peptide was released from the CNPs when subjected to low pH conditions for 24 h. The CNPs without PAA were not stable in the low pH range (3.8 and 4.2), when applying different actions (vortexing or incubation) to the CNPs at various time intervals.

An independent study demonstrated that mitomycin-C-loaded CNPs released mitomycin-C from the CNPs and sustained their release at pH levels of 6.0 and 7.4. The free drug was all released in 2 h, while release from CNPs was slower and lasted for 24 h at both pH³⁵. Table 5 further demonstrates that the CNPs rapidly discharged their payload after being exposed to the low pH buffer and incubation for 24 h, whether or not vortexing was performed, which is contrary to the earlier study by Bhardwaj et al.³⁶. Fathi et al. discovered that flurbiprofen-loaded CNPs had poor solubility at low pH, leading to poor drug release. However, they found that CNPs showed a rapid release of doxorubicin as the acidity increased³⁷. This research aimed to synthesize CNPs that are stable at low pH, ensuring prolonged and effective release of the AMP. The CNPs exhibited a burst release of Kn2-7 release within 1 h at pH 3.8 and 4.2, followed by a slow release over 24 h, with approximately 80% and 90%,

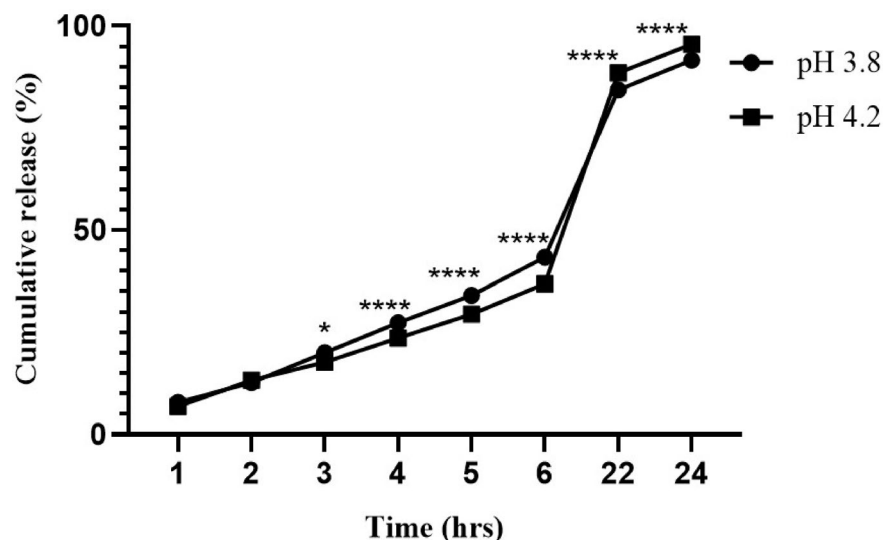


Fig. 5. Cumulative Kn2-7 peptide release profile from CNPs at pH 3.8 and pH 4.2 over 24 h. Data are presented as mean \pm SD, * $p < 0.05$, **** $p < 0.0001$.

Parameters	Kn2-7		CNPs_1mg/mLTPP-PAA	Kn2-7-CNPs_1mg/mLTPP-PAA
pH	7.4	3.8	3.8	3.8
MIC ($\mu\text{g/mL}$)	6.25	> 50	> 12.5	6.25

Table 6. MIC values as a measure for anti-bacterial activity of Kn2-7 and Kn2-7-CNPs_1mg/mL TPP-PAA.

respectively (Fig. 5). The observed release curve indicated that the CNPs_1mg/mLTPP-PAA had a potential to release their cargoes in a pH-controlled and sustained rate. pH had a strong effect on drug release that followed the same trend at the two pH levels, Kn2-7 peptide release increased over time and was slightly higher at pH 3.8. Overall, drug release depended on both pH and time, with more release seen in more acidic conditions (pH 3.8).

Antibacterial activity of Kn2-7-CNPs

The low-pH stable Kn2-7-loaded CNPs (Kn2-7-CNPs_1 mg/mLTPP-PAA) were assessed for their controlled and slow release of the AMP when subjected to low-pH environments that simulate the acidic vaginal environment. The growth kinetics of *S. aureus* at acidic conditions (pH 3.8) were not significantly different from those of the bacteria grown at normal pH (7.4) (data not shown). The Kn2-7-CNPs_1 mg/mLTPP-PAA showed better stability than the free AMP (Kn2-7 peptide) in acidic LB, and their antibacterial effect was evaluated on *S. aureus* cultured in high (7.4) and low (3.8) pH media. Kn2-7 peptide is a scorpion venom that was derived from *Buthus martensii* Karsch³⁸, it has broad-spectrum antibacterial effects in both Gram-positive and Gram-negative bacteria³⁹ including the antibiotic-resistant strains such as *Escherichia coli*, *S. aureus*, and methicillin-resistant *Staphylococcus aureus* (MRSA)¹¹. Studies have uncovered that this AMP exhibits a high level of anti-viral activity against HIV, making it a potential tool for preventing its transmission. Kn2-7 AMP inhibits microbial growth by direct interaction with microbes and is thus a promising drug candidate for the development of novel microbicidal agents^{9,40} for intra-vaginal application to prevent the transmission of STIs. One of the significant challenges for treating STIs is that the intra-vaginal environment at a pH of 3.5–4.5 is very harsh and could degrade microbicides, leading to the loss of their antimicrobial activity. In the current study, CNPs were utilized as delivery agents for the Kn2-7 peptide to protect the AMP from rapid degradation in low-pH environments.

The bacterial activity of free Kn2-7 and Kn2-7-loaded CNPs was evaluated against *S. aureus* cultured in low (pH 3.8) and high (pH 7.4) pH environments. It should be noted that *S. aureus* served as a model organism to evaluate the ability of the CNP-PAA system to deliver and protect the activity of Kn2-7 peptide within the low pH environment. The antibacterial activity of Kn2-7 peptide (0–50 $\mu\text{g/mL}$), Kn2-7-CNPs_1mg/mL TPP-PAA (6.25–50 $\mu\text{g/mL}$), and the CNPs_1mg/mL TPP-PAA (0–12.5 $\mu\text{g/mL}$) were recorded after 24 h as the Minimum Inhibitory Concentration (MIC) values. Table 6 shows that the free Kn2-7 peptide inhibited the growth of *S. aureus* at pH 7.4, with a MIC value of 6.25 $\mu\text{g/mL}$. The Kn2-7 peptide was reported to have a MIC value of 3.13 $\mu\text{g/mL}$ against *S. aureus* cultured in pH of 7.4 (normal) media¹⁸. In this study, the MIC value for Kn2-7 could not be established at pH 3.8, suggesting that the peptide's activity was affected by the low pH and failed to inhibit bacterial growth at concentrations up to 50 $\mu\text{g/mL}$. It is possible that the peptide was degraded entirely at the low pH and lost its antibacterial activity. The unloaded CNPs at concentrations ≤ 12.5 $\mu\text{g/mL}$ did not exhibit any growth inhibitory effects against *S. aureus* at either pH 3.8 or 7.4. Interestingly, the CNPs loaded with the AMP

(Kn2-7-CNPs_1 mg/mLTPP-PAA) demonstrated antibacterial activity at pH 3.8, indicating that the structure of the Kn2-7 peptide was retained even under low pH conditions.

Kn2-7-CNPs_1mg/mLTPP-PAA had a MIC value of 6.25 µg/mL at pH 3.8 that was similar to the MIC value for Kn2-7 peptide alone at pH 7.4, this implied that the antibacterial activity of Kn2-7 peptide was preserved at a low pH when loaded into the CNPs. Thus, the CNPs protected the Kn2-7 peptide from degradation, which was confirmed by the antibacterial activity of Kn2-7 peptide at pH 3.8. The MIC for CNPs_1mg/mLTPP and CNPs_1mg/mLTPP-PAA could not be determined at the concentrations tested (≤ 12.5 µg/mL) and would require concentrations > 12.5 µg/mL to induce a significant effect. This suggested that unloaded CNPs (CNPs_1mg/mL TPP-PAA) under the test conditions (both low and high pH) do not have any antibacterial activity against *S. aureus*, and that the antibacterial activity observed with the Kn2-7-CNPs_1mg/mLTPP-PAA was a result of the Kn2-7 peptide loaded onto CNPs_1mg/mL TPP-PAA. Bioactive CNPs have recently gained popularity as drug carriers and antimicrobial agents. Several researchers have studied the use of chitosan for vaginal delivery systems⁴¹, and proven to have the ability to transport drugs, peptides, and proteins across mucosal barriers⁴². Interestingly, drug-loaded CNPs had improved the mucus diffusion efficiency of protein drugs such as insulin in diabetic rats and exhibited bioavailability that was 2.8-fold higher than that of unloaded CNPs⁴³. The CNPs also ensured the controlled release of active antimicrobial agents, such as amoxicillin, from a chitosan nanocarrier compared to the commercial capsule⁴⁴. The potential of the system to be used as a vaginal microbicide delivery system could be challenged by several factors that will delay its translation into clinical applications³³. The colloidal stability of the nanocarriers must be improved by optimizing the nano-formulation to prevent early release and biodegradation of the drug. Testing against one strain (*S. aureus*) provides limited insight into the broad-spectrum efficacy required for a general vaginal microbicide. While *S. aureus* is a relevant pathogen, particularly given its increasing antibiotic resistance, a true microbicide platform would ideally demonstrate activity against a wider panel of clinically significant vaginal pathogens, including both Gram-positive and Gram-negative bacteria, as well as fungal and viral species. The relevance of this platform would also benefit from *in vitro* assays that will show their biocompatibility, mucus penetrating ability and interaction with human vaginal epithelial cells. Overall, the study demonstrated a critical step towards developing a vaginal microbicide by encapsulating Kn2-7 peptide within a CNPs-based nanocarrier that is pH-dependent.

Conclusions

The current study showed that CNPs could serve as nanocarriers for Kn2-7 peptide, the AMP when encapsulated within the CNPs was protected from degradation and was delivered intact under low pH conditions. Thus, CNPs could be suitable nanocarriers for microbicides. CNPs-based microbicides can be used as topical vaginal gels or incorporated in a condom for protection and prevention against the transmission and spread of STIs. The CNPs demonstrated stability in low pH conditions, allowing for the modulated release of their encapsulated cargoes. The findings suggested that CNPs, as drug carriers, were able to enhance the *in vitro* release profile of Kn2-7 peptide, achieving a more controlled and sustained release. The antibacterial studies demonstrated that while free Kn2-7 peptide is deactivated under acidic conditions, encapsulation within CNPs preserved its activity, even in simulated vaginal pH (approximately 3.8). The slow degradation of CNPs in this acidic environment enables the controlled release of the peptide, allowing it to exert its antibacterial effect. Encapsulating Kn2-7 peptide into CNPs protected the peptide from degradation in acidic conditions and preserved its antibacterial activity. This suggested that CNPs_1mg/mLTPP-PAA may be an effective controlled delivery system for AMPs in acidic environments like the vagina. This approach holds promise for developing microbicidal products to prevent STIs. The mucus-penetrating ability of the Kn2-7-CNPs_1mg/mLTPP-PAA still needs to be tested on artificial mucus, monitor its movement through the mucus and the time it takes to penetrate through the barrier. Their cytotoxicity effects and epithelial compatibility will be investigated in relevant vaginal models. The microbicidal activity and mechanisms of the Kn2-7-CNPs_1 mg/mLTPP-PAA will further be investigated against a panel of clinically relevant microbes, additionally, *in vivo* studies will be used to determine if the CNPs can retain controlled release and prolong the residence time of Kn2-7 peptide in animal studies.

Materials and methods

synthesis of CNPs

The synthesis of CNPs was carried out following an earlier approach as reported by Aminu Kura et al.⁴⁵ with some modifications. To prepare 2% chitosan solution, medium molecular weight chitosan (85% degree of deacetylation) (Sigma Aldrich, St Louis, MO, USA) was dissolved in 1% v/v acetic acid (Kimix, Cape Town, South Africa). The mixture was stirred with a magnetic stirrer at room temperature for 10 min. Different concentrations (0.3–5 mg/mL) of TPP (Sigma Aldrich) solution were added dropwise to the chitosan solution while stirring. The chitosan-TPP solution was sonicated on a Biobase UC-10SDII ultrasonic bath (Biobase Biodustry (Shandong) Co., Ltd., Jinan City, China) for 20 min, followed by centrifugation for 30 min at 14,500 rpm in a mini spin AG 22,331 Hamburg centrifuge (Eppendorf AG, Germany). The pellet was air-dried at room temperature.

Synthesis of Kn2-7-loaded CNPs

CNPs loaded with Kn2-7 peptide (Kn2-7-CNPs) were prepared according to the previous protocol⁴⁵. A 0.5% chitosan solution was dissolved in 1% v/v acetic acid solution and stirred at room temperature for 10 min. Kn2-7 peptide (GL Biochem, Shanghai, China) was then added to the solution and stirred for another 15 min. TPP solution at 3 mg/mL was added to the Kn2-7/chitosan solution dropwise to form the Kn2-7-CNPs-TPP. The mixture was stirred for a further 30 min. The solution was then sonicated on a Biobase UC-10SDII ultrasonic bath for 20 min, followed by three washes in water and centrifugation as before. The pellets (Kn2-7-CNPs-TPP)

were resuspended in water, then incubated at -20°C . The frozen samples were freeze-dried using the Virtis freeze dryer (SP Scientific, Gardiner, NY, USA).

Stabilization of Kn2-7-CNPs-TPP with PAA

The Kn2-7-CNPs-TPP were coated with 1800 Da PAA (Sigma Aldrich) following the layer-by-layer method described by Wu et al.⁴⁶. The Kn2-7-CNPs-TPP (0.5 mg) were added to a 1 mL solution of 10 mg/mL PAA and stirred for 1 h. The Kn2-7-CNPs_1mg/mLTPP-PAA mixture was then centrifuged at 14,500 rpm at 37°C for 30 min. The Kn2-7-CNPs_1mg/mLTPP-PAA were resuspended in 1 mL of milli-Q water, followed by ultrasonication at 45 kHz for 20 min. The samples were frozen at -20°C and freeze-dried on the Virtis freeze dryer.

Characterization of Kn2-7-CNPs

The DLS technique was employed to investigate the size distribution, polydispersity index (PDI), and zeta potential of both free and loaded CNPs using a Nano ZS Zetasizer (Malvern Panalytical Ltd., Enigma Business Park, UK). The structural features of CNPs, Kn2-7-CNPs, and Kn2-7-CNPs_1mg/mLTPP-PAA were evaluated by FTIR-410⁺ Jasco (Colchester, United Kingdom). The morphology and quality of the CNPs and Kn2-7-CNPs were investigated and captured by a Philips 400⁺ HRTEM (The Netherlands) and Tescan MIRA3 RISE scanning electron microscopy (SEM; Tescan, China) at the Electron Microscope Unit (University of Cape Town, Rondebosch, South Africa).

Loading efficiency of Kn2-7 on CNPs

The loading capacity and encapsulation efficiency were determined using a method that was previously reported by Hussein-Al-Ali et al.⁴⁵. The Kn2-7-CNPs_1mg/mLTPP-PAA obtained from "stabilization of Kn2-7-CNPs-TPP with PAA" section were aliquoted in 1.5 mL Eppendorf tubes and centrifuged for 1 h at 14,500 rpm. The supernatant was collected to quantify the amount of free Kn2-7 peptide, the absorbance was read at 210 nm on a Perkin Elmer Lambda 25 UV-visible spectrophotometer (Shelton, CT, USA). The %EE and %LC of the Kn2-7 peptide in the Kn2-7-CNPs_1mg/mLTPP-PAA were assessed by using the following equations (EQ) 1 and 2, respectively⁴⁵.

$$\%LC = \frac{A_{\text{Total peptide}} - A_{\text{Free peptide}}}{\text{NPs weight}} \times 100\% \quad (1)$$

$A_{\text{Total peptide}}$ = the absorbance of the free Kn2-7 peptide equivalent to the amount added to the reaction mixture.
 $A_{\text{Free peptide}}$ = the absorbance of the Kn2-7 peptide in the supernatant of the CNPs.
 NPs weight = the mass in mg of the CNPs that were used for loading the Kn2-7 peptide⁴⁷.

$$\%EE = \frac{A_{\text{Total peptide amount}} - A_{\text{Free peptide}}}{\text{Total peptide amount}} \times 100\% \quad (2)$$

A similar method was used to calculate %EE as in Eq. 1, however, instead of dividing by the mass of CNPs, the amount of free Kn2-7 peptide in mg was used.

Release of the Kn2-7 from CNPs

The freeze-dried Kn2-7-CNPs and Kn2-7-CNPs_1mg/mLTPP-PAA were resuspended in phosphate-buffered saline (Sigma) at varying pH conditions (3.5–4.5 and 6.0–7.4). An aliquot of 1 mL per sample was collected at 0 and 24 h, the Kn2-7 peptide concentration was quantified in the supernatants using a Qubit[™] Protein assay kit (Invitrogen, USA) following the manufacturer's instructions⁴⁸. Briefly, 1 μL of each sample, i.e., the CNPs (Kn2-7-CNPs and Kn2-7-CNPs_1mg/mLTPP-PAA) and increasing concentrations of bovine serum albumin as a standard, were individually mixed with 199 μL protein assay buffer and 1 μL protein assay reagent. The samples were incubated in the dark at room temperature for 15 min. Kn2-7 peptide concentrations were obtained using a Qubit 2.0 fluorometer (Invitrogen).

Antibacterial activity of Kn2-7 peptide and Kn2-7-CNPs

Growth kinetics of *S. aureus* in low and high pH medium

The *S. aureus* strain was purchased from the American Type Culture Collection (Manassas, VA, USA). The bacteria were cultured using a microdilution assay as described elsewhere, with a few modifications³⁹. Briefly, the bacteria were adjusted to a 0.5 McFarland turbidity standard in fresh Luria-Bertani (LB) at pH 7.4 (high) and pH 3.8 (low/acidic). The bacteria were plated at 10^6 CFU/mL without any treatments and cultured at 37°C for 24 h. Then, the growth rate of *S. aureus* at low and high pH conditions was assessed by measuring absorbance at 600 nm every hour for the first 6 hours and at 24 h using the POLARstar Omega microplate reader (Offenberger, Germany).

Determining the MIC of KN2-7 peptide and Kn2-7-CNPs

The MIC of KN2-7 peptide and Kn2-7-CNPs was evaluated on the *S. aureus* by a micro dilution assay as previously described³⁹, with some modifications. The *S. aureus* was cultured in LB at pH 3.8 and 7.4, and treated with Kn2-7 peptide, CNPs-PAA, and Kn2-7-CNPs_1mg/mLTPP-PAA. The CNPs-PAA and Kn2-7-CNPs_1mg/mLTPP-PAA were tested at concentrations ranging from 1.56 to 25 $\mu\text{g}/\text{mL}$, while the Kn2-7 peptide was tested at concentrations ranging from 3.13 to 50 $\mu\text{g}/\text{mL}$. Ciprofloxacin (Sigma Aldrich) at 5 $\mu\text{g}/\text{mL}$ was used as a

positive control. The turbidity of the bacterial suspension was visually assessed after 24 h of incubation at 37 °C as an indication of bacterial growth, and the absorbance was measured at OD 600 nm on a POLARstar Omega microplate reader. The lowest concentration of the treatments that inhibited the visible growth of bacteria was recorded as the MIC.

Statistical analysis

The data was analyzed using two-way analysis of variance (ANOVA) through GraphPad Prism version 10.6.1 (Boston, MA, USA) for statistical analysis. Sidak's multiple comparisons post hoc test was employed when significant main effects or interactions were observed to determine specific differences between group means. Statistical significance was set at $p < 0.05$ and the results are reported as mean \pm standard deviation (SD) from 3 independent experiments performed in triplicate.

Data availability

The data presented in this manuscript can be requested from the corresponding authors on reasonable request.

Received: 8 March 2025; Accepted: 23 January 2026

Published online: 05 March 2026

References

- Rosenstein, I. J. et al. Effect on normal vaginal flora of three intravaginal microbicides potentially active against human immunodeficiency virus type 1. *J. Infect. Dis.* **177**, 1386–1390. <https://doi.org/10.1086/517820> (1998).
- Sánchez-Sánchez, M. P. et al. Chitosan and Kappa-Carrageenan vaginal acyclovir formulations for prevention of genital Herpes. In vitro and ex vivo evaluation. *Mar. Drugs*. **13**, 5976–5992. <https://doi.org/10.3390/md13095976> (2015).
- Lund, P., Tramonti, A. & De Biase, D. Coping with low pH: molecular strategies in neutralophilic bacteria. *FEMS Microbiol. Rev.* **38**, 1091–1125. <https://doi.org/10.1111/1574-6976.12076> (2014).
- Nakano, F. Y., Leão, R. & de BF, Esteves, S. C. Insights into the role of cervical mucus and vaginal pH in unexplained infertility. *Med. Express*. **2**, 1–8. <https://doi.org/10.5935/MedicalExpress.2015.02.07> (2015).
- Hmed, B., Serria, H. T. & Mounir, Z. K. Scorpion peptides: potential use for new drug development. *J. Toxicol.* **2013**, 1–15. <https://doi.org/10.1155/2013/958797> (2013).
- Notario-Pérez, F., Ruiz-Caro, R. & Veiga-Ochoa, M. D. Historical development of vaginal microbicides to prevent sexual transmission of HIV in women: from past failures to future hopes. *Drug Des. Devel Ther.* **11**, 1767–1787. <https://doi.org/10.2147/DDDT.S133170> (2017).
- Cutler, B. & Justman, J. Vaginal microbicides and the prevention of HIV transmission. *Lancet Infect. Dis.* **8**, 685–697. [https://doi.org/10.1016/S1473-3099\(08\)70254-8](https://doi.org/10.1016/S1473-3099(08)70254-8) (2008).
- Choudhury, A., Das, S. & Kar, M. A review on novelty and potentiality of vaginal drug delivery. *Int. J. PharmTech Res.* **3**, 1033–1044 (2011).
- Lei, J. et al. The antimicrobial peptides and their potential clinical applications. *Am. J. Transl. Res.* **11**: 3919–3931. (2019).
- Fadaka, A. O., Sibuyi, N. R. S., Madiehe, A. M. & Meyer, M. Nanotechnology-based delivery systems for antimicrobial peptides. *Pharmaceutics* **13** <https://doi.org/10.3390/pharmaceutics13111795> (2021).
- Chen, Y. et al. Anti-HIV-1 activity of a new Scorpion venom peptide derivative Kn2-7. *J. Nat. Prod.* **7**: 1–9. (2012). <https://doi.org/10.1371/journal.pone.0034947>
- Inthanachai, T. et al. The inhibitory effect of human Beta-defensin-3 on *Candida glabrata* isolated from patients with candidiasis. *Immunol. Invest.* **50**, 80–91. <https://doi.org/10.1080/08820139.2020.1755307> (2021).
- Pauwels, R. & De Clercq, E. Development of vaginal microbicides for the prevention of heterosexual transmission of HIV. *J. Acquir. Immune Defic. Syndr. Hum. Retrovirology*. **11**, 211–221. <https://doi.org/10.1097/00042560-199603010-00001> (1996).
- Kumari, P., Ghosh, B. & Biswas, S. Nanocarriers for cancer-targeted drug delivery. *J. Drug Target.* **24**, 179–191. <https://doi.org/10.3109/1061186X.2015.1051049> (2016).
- Debi Prasanna, M., Yogesh, P., Palve, D. & Sahoo, Nayak, P. L. Synthesis and characterization of Chitosan/Cloisite 30B (MMT) nanocomposite for controlled release of anticancer drug Curcumin. *Int. J. Pharm. Res. Allied Sci.* **1**, 52–62 (2012).
- Robertson, J. 11119. *Am Math Mon.* **111**: 915. (2004). <https://doi.org/10.2307/4145104>
- Qi, L., Xu, Z., Jiang, X., Hu, C. & Zou, X. Preparation and antibacterial activity of Chitosan nanoparticles. *J. Pharm. Res.* **339**: 2693–2700. (2004). <https://doi.org/10.1016/j.carres.2004.09.007>
- Kean, T. & Thanou, M. Biodegradation, biodistribution and toxicity of Chitosan. *Adv. Drug Deliv Rev.* **62**, 3–11. <https://doi.org/10.1016/j.addr.2009.09.004> (2010).
- Filippov, S. K. et al. Dynamic light scattering and transmission electron microscopy in drug delivery: a roadmap for correct characterization of nanoparticles and interpretation of results. *Mater. Horizons*. **10**, 5354–5370. <https://doi.org/10.1039/d3mh00717k> (2023).
- Bodnar, M., Hartmann, J. F. & Borbely, J. Preparation and characterization of chitosan-based nanoparticles. *Biomacromolecules* **6**, 2521–2527. <https://doi.org/10.1021/bm0502258> (2005).
- Honary, S. & Zahir, F. Effect of zeta potential on the properties of Nano-Drug delivery Systems - A review (Part 1). *Trop. J. Pharm. Res.* **12**, 255–264 (2013).
- Banerjee, T., Mitra, S., Kumar Singh, A., Kumar Sharma, R. & Maitra, A. Preparation, characterization and biodistribution of ultrafine Chitosan nanoparticles. *Int. J. Pharm.* **243**, 93–105. [https://doi.org/10.1016/S0378-5173\(02\)00267-3](https://doi.org/10.1016/S0378-5173(02)00267-3) (2002).
- Eskandari, N. M. D., Zolfagharian, R. & Mohammad, H. Preparation and in vitro characterization of Chitosan nanoparticles containing mesobuthus Eupeus Scorpion venom as an antigen delivery system. *J. Venom. Anim. Toxins Incl. Trop. Dis.* **18**, 44–52. <https://doi.org/10.1590/S1678-91992012000100006> (2012).
- Gimondi, S., Ferreira, H., Reis, R. L. & Neves, N. M. Intracellular trafficking of Size-Tuned nanoparticles for drug delivery. *Int. J. Mol. Sci.* **25** <https://doi.org/10.3390/ijms25010312> (2024).
- Vedantam, P., Huang, G. & Tzeng, T. R. J. Size-dependent cellular toxicity and uptake of commercial colloidal gold nanoparticles in DU-145 cells. *Cancer Nanotechnol.* **4**, 13–20. <https://doi.org/10.1007/s12645-013-0033-8> (2013).
- Hoshyar, N., Gray, S., Han, H. & Bao, G. The effect of nanoparticle size on in vivo pharmacokinetics and cellular interaction. *Nanomedicine* **11**, 673–692. <https://doi.org/10.2217/nmm.16.5> (2016).
- Wang, Z. L. New developments in transmission electron microscopy for nanotechnology. *Adv. Mater.* **15**, 1497–1514. <https://doi.org/10.1002/adma.200300384> (2003).
- Kiillil, C. P. et al. Synthesis and factorial design applied to a novel chitosan/sodium polyphosphate nanoparticles via ionotropic gelation as an RGD delivery system. *Carbohydr. Polym.* **157**, 1695–1702. <https://doi.org/10.1016/j.carbpol.2016.11.053> (2017).
- Hasheminejad, N., Khodaiyan, F. & Safari, M. Improving the antifungal activity of clove essential oil encapsulated by Chitosan nanoparticles. *Food Chem.* **275**, 113–122. <https://doi.org/10.1016/j.foodchem.2018.09.085> (2019).

30. Amidi, M. et al. Preparation and characterization of protein-loaded N-trimethyl Chitosan nanoparticles as nasal delivery system. *J. Control Release*. **111**, 107–116. <https://doi.org/10.1016/j.jconrel.2005.11.014> (2006).
31. Khan, S. & Anwar, N. Highly porous pH-Responsive carboxymethyl Chitosan- grafted -Poly (Acrylic Acid) based smart hydrogels for 5-Fluorouracil controlled delivery and colon targeting. *Int. J. Polym. Sci.* **2019**, 1–15. <https://doi.org/10.1155/2019/6579239> (2019).
32. Elfadil, D., Elkhatib, W. F., El-sayyad, G. S. & Nps, A. Microbial pathogenesis promising advances in nanobiotic-based formulations for drug specific targeting against multidrug-resistant microbes and biofilm-associated infections. *Microb. Pathog.* **170**, 105721. <https://doi.org/10.1016/j.micpath.2022.105721> (2022).
33. Chakraborty, N., Jha, D., Roy, I., Kumar, P. & Gaurav, S. S. Nanobiotics against antimicrobial resistance: Harnessing the power of nanoscale materials and technologies. *J. Nanobiotechnol.* **20**, 375. <https://doi.org/10.1186/s12951-022-01573-9> (2022).
34. Grenha, A., Seijo, B. & Remuñán-López, C. Microencapsulated Chitosan nanoparticles for lung protein delivery. *Eur. J. Pharm. Sci.* **25**, 427–437. <https://doi.org/10.1016/j.ejps.2005.04.009> (2005).
35. Kavaz, D., Kirac, F., Kirac, M. & Vaseashta, A. Low releasing mitomycin C molecule encapsulated with Chitosan nanoparticles for intravesical installation. *J. Biomater. Nanobiotechnol.* **08**, 203–219. <https://doi.org/10.4236/jbnb.2017.84014> (2017).
36. Bhardwaj, P. & Singh, S. Formulation and in vitro evaluation of pH-sensitive Chitosan beads of flurbiprofen. *Indian Journal of Drugs*. **1**, 48–54. (2013).
37. Fathi, M. et al. Stimuli-responsive chitosan-based nanocarriers for cancer therapy. *Bioimpacts*. **7**, 269–277. (2017). <https://doi.org/10.15171/bi.2014.008>
38. Hui Zhang, J. W. Review on bioactive peptides and Pharmacological activities of *Buthus martensii* Karsch. *Biochem. Pharmacol.* **4** (2). <https://doi.org/10.4172/2167-0501.1000166> (2015).
39. Cao, L. et al. Antibacterial activity and mechanism of a Scorpion venom peptide derivative in vitro and in vivo. *PLoS One*. **7**, (2012). <https://doi.org/10.1371/journal.pone.0040135>
40. Malcolm, R. K., Woolfson, A. D., Toner, C. F., Morrow, R. J. & Mccullagh, S. D. Long-term, controlled release of the HIV microbicide TMC120 from silicone elastomer vaginal rings. *J. Antimicrob. Chemother.* **56**, 954–956. (2005). <https://doi.org/10.1093/jac/dki326>
41. Tuğcu-Demiröz, F. et al. Development and characterization of Chitosan nanoparticles loaded nanofiber hybrid system for vaginal controlled release of benzydamine. *Eur. J. Pharm. Sci.* **161**, 105801. <https://doi.org/10.1016/j.ejps.2021.105801> (2021).
42. Zambito, Y. Nanoparticles based on Chitosan derivatives. *Advances in Biomaterials Science and Biomedical Applications*, Ed Pignatello R, pp 243–263. <https://doi.org/10.5772/54944> (2013).
43. Liu, M. et al. Efficient mucus permeation and tight junction opening by dissociable mucus-inert agent coated trimethyl Chitosan nanoparticles for oral insulin delivery. *J. Control Release*. **222**, 67–77. <https://doi.org/10.1016/j.jconrel.2015.12.008> (2016).
44. Sahasathian, T. et al. Sustained release of amoxicillin from Chitosan tablets. *Arch. Pharm. Res.* **30**, 526–531. <https://doi.org/10.1007/BF02980229> (2007).
45. Hussein-al-ali, S. H., Kura, A., Hussein, M. Z. & Fakurazi, S. Preparation of Chitosan nanoparticles as a drug delivery system for Perindopril erbumine. *Polym. Compos.* **59**, 544–552. <https://doi.org/10.1002/pc.23967> (2016).
46. Wu, Y. et al. Facile fabrication of poly(acrylic acid) coated Chitosan nanoparticles with improved stability in biological environments. *Eur. J. Pharm. Biopharm.* **112**, 148–154. <https://doi.org/10.1016/j.ejpb.2016.11.020> (2017).
47. Saeed, R. M., Dmour, I. & Taha, M. O. Stable Chitosan-Based nanoparticles using polyphosphoric acid or hexametaphosphate for tandem Iontropic/Covalent crosslinking and subsequent investigation as novel vehicles for drug delivery. *Front. Bioeng. Biotechnol.* **8**, 4. <https://doi.org/10.3389/FBIOE.2020.00004/BIBTEX> (2020).
48. Id, Z. D. et al. Application of BisANS fluorescent dye for developing a novel protein assay. *PLoS One*. **14**, e0215863. <https://doi.org/10.1371/journal.pone.0215863> (2019).

Acknowledgements

The research data presented herein is part of Dr Bonke Phathekile's MSc project “Synthesis of peptide-loaded chitosan nanoparticles for the treatment of sexually transmitted infections (STTs), 2020” that is available on the university website.

Author contributions

SM, AMM, GEO, MOO and MM - Conceptualization, resources, supervision, funding acquisition; BP and NRSS - methodology, project administration, formal analysis, investigation and data curation; BP - writing-original draft preparation; NRSS, SM, AMM, GEO, MOO and MM - writing-review and editing. All authors have read and agreed to the published version of the manuscript.

Funding

This research was funded by NRF-Thuthuka Rating Track, Grant number TTK150625121238; UID: 99307 and UWC Natechnology platform.

Declarations

Competing interests

The authors declare no competing interests.

Additional information

Correspondence and requests for materials should be addressed to N.R.S.S., M.O.O. or M.M.

Reprints and permissions information is available at www.nature.com/reprints.

Publisher's note Springer Nature remains neutral with regard to jurisdictional claims in published maps and institutional affiliations.

Open Access This article is licensed under a Creative Commons Attribution-NonCommercial-NoDerivatives 4.0 International License, which permits any non-commercial use, sharing, distribution and reproduction in any medium or format, as long as you give appropriate credit to the original author(s) and the source, provide a link to the Creative Commons licence, and indicate if you modified the licensed material. You do not have permission under this licence to share adapted material derived from this article or parts of it. The images or other third party material in this article are included in the article's Creative Commons licence, unless indicated otherwise in a credit line to the material. If material is not included in the article's Creative Commons licence and your intended use is not permitted by statutory regulation or exceeds the permitted use, you will need to obtain permission directly from the copyright holder. To view a copy of this licence, visit <http://creativecommons.org/licenses/by-nc-nd/4.0/>.

© The Author(s) 2026